Protein Expression and Purification 109 (2015) 7–13

Contents lists available at ScienceDirect

Protein Expression and Purification

journal homepage: www.elsevier.com/locate/yprep

Expression and purification of soluble and stable ectodomain of natural killer cell receptor LLT1 through high-density transfection of suspension adapted HEK293S GnTI$^-$ cells

Jan Bláha [a], Petr Pachl [b], Petr Novák [a,c], Ondřej Vaněk [a,*]

[a] Department of Biochemistry, Faculty of Science, Charles University in Prague, Hlavova 8, Prague 12840, Czech Republic
[b] Institute of Organic Chemistry and Biochemistry, Academy of Sciences of the Czech Republic, Flemingovo nám. 2, Prague 16610, Czech Republic
[c] Institute of Microbiology, Academy of Sciences of the Czech Republic, Vídeňská 1083, Prague 14220, Czech Republic

ARTICLE INFO

Article history:
Received 12 December 2014
and in revised form 15 January 2015
Available online 24 January 2015

Keywords:
LLT1
HEK293S GnTI$^-$
C-type lectin-like
NK cell
Glycosylation
Transfection

ABSTRACT

Lectin-like transcript 1 (LLT1, gene *clec2d*) was identified to be a ligand for the single human NKR-P1 receptor present on NK and NK-T lymphocytes. Naturally, LLT1 is expressed on the surface of NK cells, stimulating IFN-γ production, and is up-regulated upon activation of other immune cells, e.g. TLR-stimulated dendritic cells and B cells or T cell receptor-activated T cells. While in normal tissues LLT1:NKR-P1 interaction (representing an alternative "missing-self" recognition system) play an immunomodulatory role in regulation of crosstalk between NK and antigen presenting cells, LLT1 is upregulated in glioblastoma cells, one of the most lethal tumors, where it acts as a mediator of immune escape of glioma cells.

Here we report transient expression and characterization of soluble His176Cys mutant of LLT1 ectodomain in an eukaryotic expression system of human suspension-adapted HEK293S GnTI$^-$ cell line with uniform N-glycans. The His176Cys mutation is critical for C-type lectin-like domain stability, leading to the reconstruction of third canonical disulfide bridge in LLT1, as shown by mass spectrometry. Purified soluble LLT1 is homogeneous, deglycosylatable and forms a non-covalent homodimer whose dimerization is not dependent on presence of its N-glycans.

As a part of production of soluble LLT1, we have adapted HEK293S GnTI$^-$ cell line to growth in suspension in media facilitating transient transfection and optimized novel high cell density transfection protocol, greatly enhancing protein yields. This transfection protocol is generally applicable for protein production within this cell line, especially for protein crystallography.

Introduction

Natural killer (NK[1]) cells are large granular lymphocytes that are able to destroy tumor, virally infected or stressed cells based on equilibrium between stimulatory and inhibitory signals mediated by their surface recognition receptors [1]. While the role of some NK cell receptors in antitumor immunity is described in relatively great detail, on the other hand, the possible utilization of soluble receptor domains in antitumor therapy is only beginning to be explored. The main NK cell activating receptors studied in this respect include C-type lectin-like NKG2D receptor and immunoglobulin-like receptor NKp30 [1]. For example, the soluble NKp30–Fc_IgG fusion protein was shown to inhibit the growth of prostate cancer cell line *in vivo*, including complete tumor removal in 50% of mice [2]. In another study, a synergy was observed when bifunctional anti-CD20 scFv fusions with natural ligands for NKp30 and NKG2D receptors were combined [3] and it could be expected that further increase in antitumor potency might be reached by simultaneous targeting of other activation or co-stimulatory receptors, e.g. NKp80, NKp65 or LLT1. Therefore technologies leading to production of soluble domains of these receptors as well as of their ligands in good yield and stability are needed.

Lectin-like transcript 1 (LLT1, gene *clec2d*) is a type II transmembrane receptor belonging to the C-type lectin like (CTL) superfamily of natural killer cell receptors. Six alternatively spliced transcripts of *clec2d* gene were identified, with the isoform 1

* Corresponding author at: Department of Biochemistry, Faculty of Science, Charles University in Prague, Hlavova 2030, Prague 12840, Czech Republic. Tel.: +420 22195 1272; fax: +420 22195 1283.
E-mail address: ondrej.vanek@natur.cuni.cz (O. Vaněk).

[1] *Abbreviations used:* CTL, C-type lectin-like; dpt, days post-transfection; GFP, green fluorescent protein; GnTI$^-$, N-acetylglucosaminyltransferase I negative; HEK, human embryonic kidney; NK, natural killer; LLT1, lectin-like transcript 1; lPEI, linear polyethylenimine; PBS, phosphate buffered saline; pNPP, *p*-nitrophenyl phosphate; SEAP, secreted alkaline phosphatase; SEC, size exclusion chromatography; WT, wild-type.

http://dx.doi.org/10.1016/j.pep.2015.01.006
1046-5928/

(designated as LLT1) being the only one presented on the cell surface, thus being the only isoform able to participate in the cell to cell signal transmission [4]. LLT1 is expressed mainly on activated lymphocytes (NK cells, T cells, B cells) and antigen presenting cells, i.e. macrophages and dendritic cells [5].

Almost a decade ago, LLT1 was identified as a physiological ligand of NKR-P1 (CD161, gene *klrb1*) – the only described representative of human NKR-P1 subfamily [6,7]. NK cell cytotoxicity and IFNγ production is inhibited upon engagement of NKR-P1 on NK cell with LLT1 on target cell [6,7]. It has been shown that this mechanism contributing to NK self-tolerance is being exploited by the human glioblastoma cells that are escaping the appropriate immunological response by up-regulating the surface expression of LLT1 [8]. However, in response to microbial and viral stimuli LLT1 expression is up-regulated on surface of epithelial cells [9], and also IFNγ increases LLT1 expression on B cells and antigen presenting cells [5]. Upon ligation with CD161 these cells can co-stimulate T cell proliferation, cytokine secretion and proinflammatory responses. Therefore LLT1:NKR-P1 signalization represents a system that regulates both innate and adaptive immune responses and may provide a link between pathogen pattern recognition and lymphocyte activation [9].

The polypeptide chain of LLT1 can be divided into the N-terminal cytoplasmic part, transmembrane and stalk regions and C-terminal CTL ectodomain with two predicted N-glycosylation sites. While homologous CTL receptors usually contain two or three canonical disulfide bonds corresponding to four or six cysteines within their CTL domain, respectively [10], the CTL domain of LLT1 contains five conserved cysteine residues. Thus, two putative canonical disulfide bridges (Cys75–Cys86 and Cys103–Cys184) may be formed leaving Cys163 unpaired. Previously [11] reported that the mutation of His176 residue to Cys176 improves on stability of recombinant LLT1 ectodomain expressed in *Escherichia coli* and refolded from inclusion bodies *in vitro*, hence proposing that this mutation might reconstruct the third disulfide bridge.

Here we report a transient gene expression of LLT1 ectodomain H176C mutant in suspension adapted HEK293S N-acetylglucosaminyltransferase I negative (GnTI$^-$) cell line, originally developed for expression of rhodopsin mutants [12], that provides recombinant proteins with homogeneous $GlcNAc_2Man_5$ N-linked oligosaccharides, making them excellent for structural and biophysical studies. Unfortunately this quality is often repaid by lower yields of protein [13]. Current production protocols reported so far are based either on rather slow generation of stably transfected cell lines [12] or transient transfection using adherent cell culture which might get laborious and material consuming when scaling-up with the yields reportedly being lower when compared to other HEK293 cell line derivatives, e.g. HEK293T or HEK293E [14]. In order to improve the transfection efficiency and productivity of HEK293S GnTI$^-$ cell line we have adapted these cells to growth in suspension and optimized for them a high-density transfection protocol previously reported for HEK293E cells [15–17], thus greatly enhancing the protein yields when compared to standard low-density transfection. This transfection protocol is generally applicable for protein production within this cell line, especially for protein crystallography.

Materials and methods

Vectors and cloning

The pTTo3c_SSH and pTTo_GFPq vectors containing SEAP and GFP, respectively, were kindly provided by Dr. Yves Durocher [18] as well as pT28 plasmid, a derivative of pTT5 [18] containing N-terminal secretion leader and C-terminal His_8-tag sequence (leaving ITG- and -GTKHHHHHHHHG at expressed protein N- and C-termini), whose multiple cloning site was further modified to include AgeI and KpnI restriction sites. Total RNA was isolated from human spleen with TRIzol and used as template for single stranded cDNA synthesis using Superscript III reverse transcriptase (both Invitrogen, USA). DNA fragment coding for LLT1 was amplified using 5′ TGCAAGCTGCATGCCCAGAAAG 3′ and 5′ CCTCGA GCTAGACATGTATATCTGATTTGGA 3′ primers and the PCR product was subcloned into the SmaI site of pBluescript SK + cloning vector (Stratagene, USA). The extracellular portion of LLT1 (Q72-V191) was amplified from the cloning vector using 5′ AAAAAAACC GGTCAAGCTGCATGCCCAGAAAGC 3′ and 5′ AAAAAAGGTACCGAC ATGTATATCTGATTTGGAACAAATC 3′ primers and subcloned into the pTT28 expression plasmid using AgeI and KpnI sites. Mutant constructs of LLT1 were prepared by overlap extension PCR [19,20], using the prepared expression plasmid as template and aforementioned primers as forward and reverse primers. The specific forward primers used for preparation of C163S and H176C mutants have been 5′ GAGCAGGAGAGTCTGCCTATTTGAA 3′ and 5′ GTAGTGCCAGGTGCTACACAGAGAG 3′, respectively.

Cell culture

The HEK293T cells were kindly provided by Dr. Radu A. Aricescu [14]. The HEK293S GnTI$^-$ cell line was purchased from ATCC (CRL-3022) [12]. These adherent cultures were firstly adapted to growth in EX-CELL293 serum-free medium (Sigma, USA) supplemented with 4 mM L-glutamine on Petri dishes by consecutive subcultivations until the cells resumed normal growth rate (doubling time approx. 24 h) and later were adapted to growth in suspension in mixture of equal volumes of EX-CELL293 supplemented as above and Freestyle F17 (Invitrogen, USA) supplemented with 4 mM L-glutamine and 0.1% Pluronic F-68 (Sigma, USA) in shaken square-shaped glass bottles with permeable filter caps (DURAN, Germany) using 30-40% filling volume at 135 rpm (Orbit1000 shaker; Labnet, USA) in humidified 37 °C, 5% CO_2 incubator. The cell density was kept between 0.2 and 6.0 × 10^6 cells/ml.

Low-scale transfection

Day before transfection cells were centrifuged and resuspended in fresh supplemented F17 medium (1.0 × 10^6 cells/ml). Next day, cell density was adjusted to 2.0 × 10^6 cells/ml and 1 ml was distributed per well in 12-well plate. Transfection mix was prepared by diluting DNA (1 μg/10^6 cells) to 0.1 ml PBS (1/10 transfection culture volume), 1 mg/ml solution of 25 kDa linear polyethylenimine (lPEI; Polysciences, USA) was added to desired ratio, the mixture was immediately vigorously shaken and following 5 min incubation added to the cell suspension. After 4 h incubation the suspension was diluted with 1 ml of EX-CELL293 to 1.0 × 10^6/ml final density. For high-density transfection the cells were prepared on the day of transfection. Cells were centrifuged and resuspended in fresh supplemented EX-CELL293 medium (25 × 10^6 cells/ml) and 0.4 ml was distributed per well in 12-well plate. The suspension was then diluted with approximately 0.1 ml of transfection mix (prepared as above) to 20 × 10^6 cells/ml. After 4 h incubation 0.1 ml of this suspension was diluted with 1.9 ml of EX-CELL293 in new 12-well plate to final density of 1.0 × 10^6/ml.

SEAP and GFP analysis

Determination of SEAP activity (ΔA_{410}/min) was performed as previously described [18]. Briefly, HEK293 cells were transfected with 19:1 (w/w) mixture of pTTo3c_SSH and pTTo_GFPq plasmids. Three dpt culture supernatants were diluted with water as required (typically 1/1000), 180 μl were transferred to 96-well

plate, 20 μl of SEAP assay solution (20 mM *p*-nitrophenyl phosphate (pNPP), 1 mM $MgCl_2$ and 1 M diethanolamine, pH 9.8) were added and absorbance was read at 410 nm at 1 min intervals to determine pNPP hydrolysis rates (Safire reader; Tecan, Austria). Each sample was assayed for SEAP activity three times independently to avoid pipetting errors. Transfection efficiency was assayed by BD LSR II flow cytometer (BD Biosciences, USA). GFP-positive viable cells were quantified by using appropriate gating to exclude dead cells (stained with propidium iodide), debris and aggregates in forward vs. side scatter plot. Data are shown as mean of one experiment performed in triplicate with error bars representing standard deviation.

Protein production and purification

For LLT1 production, 400 μg of the respective expression plasmid was diluted in PBS, filter-sterilized and 25 kDa lPEI was added in 1:3 weight ratio to final volume of 4 ml, the mixture was shaken and incubated for 5 min. Meanwhile, 400×10^6 HEK293S GnTI$^-$ cells were centrifuged and resuspended in EX-CELL293 (if not specified otherwise) at 25×10^6 cells/ml and immediately transfected. Following 4 h incubation culture was diluted to 400 ml with EX-CELL293. Two dpt, culture was fed with 0.5% Tryptone N1 (Organotechnie, France) [21]. 5-7 dpt culture medium was harvested by centrifugation (4000×*g*, 30 min), filtered (0.22 μm Steritop filter; Millipore, USA), and stored at −20 °C or immediately processed. Medium was diluted twofold with PBS (50 mM Na_2HPO_4, 300 mM NaCl, 10 mM NaN_3) and pH was adjusted to 7.0. The protein was recovered by batch IMAC chromatography on TALON beads (Clontech, USA; elution by 250 mM imidazole within the PBS buffer) with subsequent SEC on Superdex 200 10/300 GL column (GE Healthcare, USA) in 10 mM HEPES, 150 mM NaCl, 10 mM NaN_3, pH 7.5 buffer and concentrated on AmiconUltra concentrator (10,000 MWCO; Millipore, USA).

Sedimentation analysis

Molecular weight of the produced protein was analyzed in an analytical ultracentrifuge ProteomeLab XL-I equipped with An-50 Ti rotor (BeckmanCoulter, USA) using sedimentation equilibrium experiment. Native and deglycosylated LLT1(H176C) diluted with SEC buffer to 0.07 and 0.09 mg/ml, respectively, were measured at 4 °C using absorbance optics at 280 nm in 0.11 ml total volume at 12–15–18–21–24–27–30,000 rpm after reaching the equilibrium for 18 h at each given speed. Buffer density and protein partial specific volume were estimated in Sednterp 1.09 (www.jphilo.mailway.com). The data were analyzed using Sedphat 10.58d software [22] using single non-interacting discrete species model.

Mass spectrometry

Disulfide bonds in LLT1 were determined according to the previously published protocol [23]. Briefly, the protein was separated by SDS–PAGE, deglycosylated by ENDO Hf (New England Biolabs, USA) and digested by trypsin (Sigma, USA) under non-reducing conditions in the presence of 200 μM cystamine. The peptide mixtures were desalted on peptide MacroTrap and separated on reverse phase MAGIC C18 columns (both Michrom BioResources, USA) connected directly to an APEX-Q 9.4 T FT-ICR mass spectrometer (Bruker Daltonics, USA) using an electrospray ion source. Data were acquired using ApexControl 3.0.0 and processed with DataAnalysis 4.0. The disulfide bonds and saccharide moieties were identified using Links software [24].

Protein crystallization

LLT1 solution concentrated to 13.8 mg/ml was crystallized using vapor diffusion method in sitting drop (50 μl reservoir volume). Drops were set up by crystallization robot Crystal Gryphon (Art Robbins Instruments, USA) by mixing 200 nl of both reservoir (JCSG + Suite; Qiagen, USA) and protein solutions at 15 °C. The successful crystallization condition reservoir contained 40% (v/v) PEG 300 and 0.1 M citrate phosphate buffer (pH 4.2). Rod shaped crystals of approximately $150 \times 50 \times 50$ μm in size grew within 14 days.

Results and discussion

Reconstruction of third disulfide bridge is crucial for stability of LLT1 ectodomain

The C-type lectin-like ectodomain of LLT1 contains five cysteine residues and the multiple alignment analysis shows that only two out of three putative disulfide bonds are thus conceivable, with Cys163 residue left unpaired (Fig. 1A). Earlier it has been proposed that mutation of His176 to Cys176 leads to reconstruction of the third disulfide bridge [11]. Initially, we have produced the wild-type (WT) LLT1 ectodomain (Q72-V191) in HEK293T cells; however the purified protein was heterogeneous and was prone to aggregation (Fig. 1B). Based on these results and assumptions we have prepared C163S and H176C mutant forms of soluble LLT1 ectodomain. While the mutation of odd Cys163 residue to Ser163 led to very low yield of recoverable product, the mutation of His176 to Cys176 led to monodisperse and stable product (Fig. 1B). These findings correlate very well with previously reported data of unstable WT and C163S mutant LLT1 ectodomain renaturated from *E. coli* expressed inclusion bodies [11] and suggest structurally stabilizing role of the third disulfide bridge in LLT1(H176C) ectodomain.

Furthermore, using mass spectrometry approach [23] we were able to identify the cystine peptides in the H176C mutant and WT soluble LLT1. While in case of WT we have observed quite heterogeneous configuration of disulfide bridges with majority of Cys163 participating in covalent bond with Cys184 and only very small percentage left unpaired (supplementary data, Table S1), we were able to confirm the reconstruction of Cys163–Cys176 putative disulfide bridge in H176C mutant protein (Fig. 1C and supplementary data, Table S2). Moreover, we were able to confirm the presence of saccharide moiety at both predicted N-glycosylation sites (Fig. 1A and supplementary data, Table S2). The incomplete occupancy of these two possible sites accounts for two different glycoforms as observed on SDS–PAGE (see below).

High-density transfection of HEK293S GnTI$^-$ cells substantially improves transfection efficiency and expression yields

In order to produce glycosylated ectodomain of LLT1 with homogeneous N-glycans for structural and biophysical studies we have investigated the optimal transfection conditions for suspension adapted HEK293S GnTI$^-$ cell line [12], based on previously published transfection protocols for suspension adapted HEK293E cells [15,18]. The adherent HEK293S GnTI$^-$ and HEK293T cultures were adapted to growth in suspension in equal mixture of serum-free EX-CELL293 and Freestyle F17 media in shaken square bottles, as described in methods (2.2). For evaluation of transfection efficiency and production of secreted recombinant protein we have used previously adopted reporter genes – green fluorescent protein (GFP) and secreted alkaline phosphatase (SEAP), respectively [18]. Initially we have found that protocol optimized

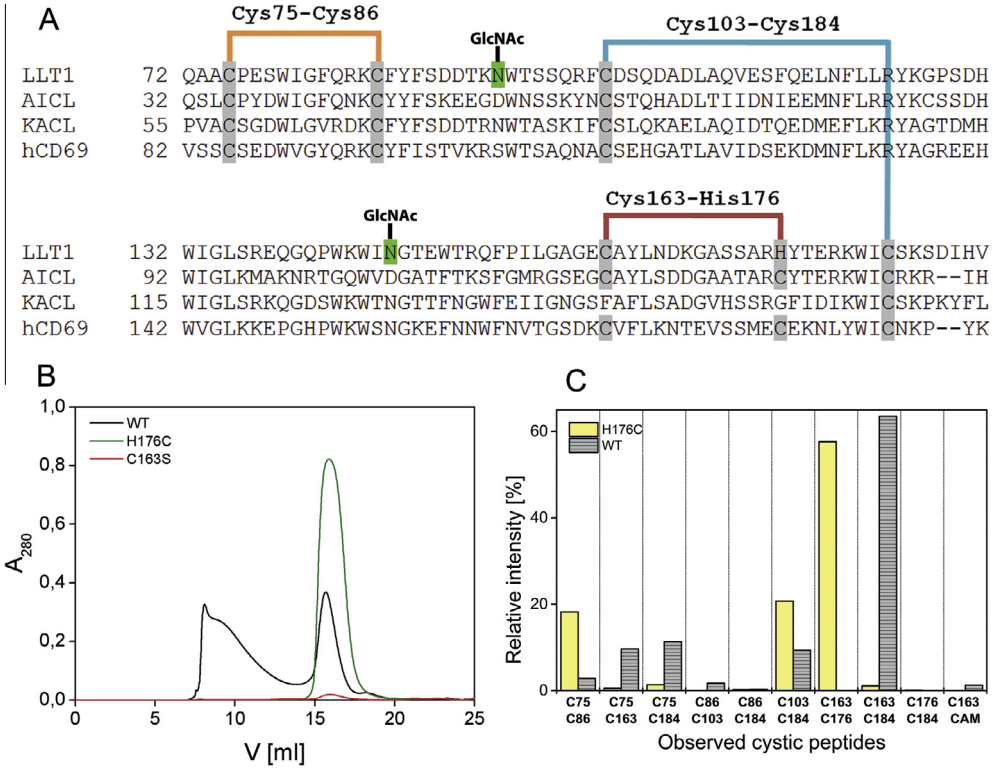

Fig. 1. The reconstruction of disulfide bridge improves folding and yield of soluble LLT1. (A) Multiple sequence alignment of C-type lectin-like domain sequences of receptors from human *clec2* gene family showing conserved cysteines in gray and their disulfidic pairing; reconstructed disulfide bridge in LLT1(H176C) mutant is high-lighted in red and N-glycosylation sites in green. (B) Size exclusion chromatography of soluble LLT1 wild-type (black) and mutant H176C (green) and C163S (red) proteins produced in HEK293T cell line. (C) Mass spectrometry analysis of disulfide bond pattern in wild-type and LLT1(H176C) mutant; proteins produced in HEK293S GnTI$^-$ cell line were purified by IMAC and SEC chromatography and samples corresponding to peak at 16 ml position on SEC run shown in B were deglycosylated, digested and the resultant cystic peptides were analyzed by FT-ICR MS as described in methods, the relative intensity of observed cystic peptides (error below 3 ppm) is shown. (For interpretation of the references to color in this figure legend, the reader is referred to the web version of this article.)

for suspension adapted HEK293T cells used routinely in our laboratory – transfection at density of 2.0×10^6 cells/ml in Freestyle F17 (medium exchanged one day prior to transfection), transfection complexes formed *a priori* with 2 μg/ml of DNA (final concentration) at optimal 1:3 DNA:PEI weight to weight ratio – was quite inefficient for transfection of HEK293S GnTI$^-$ cells (Fig. 2, yellow vs. cyan columns).

The obvious difference between the HEK293T and HEK293S GnTI$^-$ cells is the lack of complex glycans resulting also in loss of a sulfated negatively charged glycans displayed at the cell surface that might attract positively charged DNA:PEI polyplexes. We have thus theorized that by increasing the concentration of DNA and PEI during the transfection process we could improve the transfection efficiency. This prompted us to test the previously reported protocol for transient transfection of suspension adapted HEK293E cells in EX-CELL293 medium at high cell density [15]. Interestingly, transfection of HEK293S GnTI$^-$ cells at high cell density (20×10^6 cells/ml in EX-CELL293 with final DNA concentration of 20 μg/ml) proved to be much more efficient with up to 5-fold increase in transfection efficiency measured as percentage of GFP positive

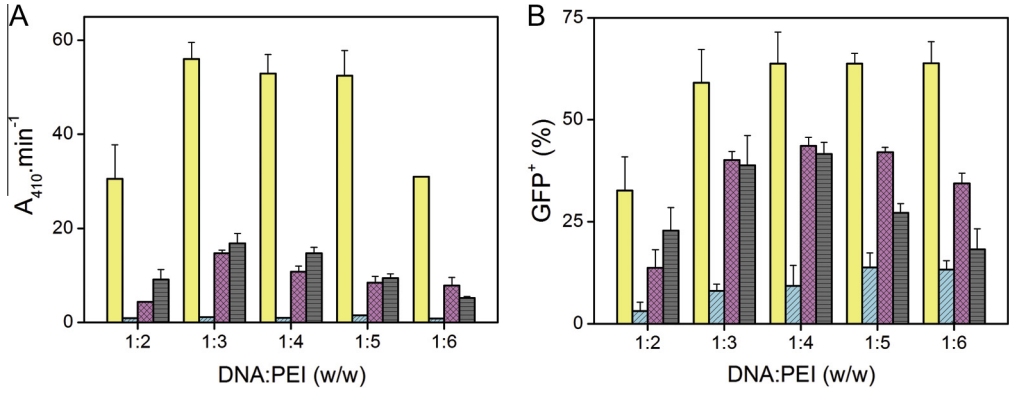

Fig. 2. High-density transfection of HEK293SGnTI$^-$ cells under optimized DNA:PEI ratio increases transfection efficiency and cell productivity. (A) Secreted protein production (measured as SEAP activity) and (B) transfection efficiency (GFP$^+$ viable cells) of suspension adapted HEK293T cells (yellow) and HEK293S GnTI$^-$ cells (cyan) transfected at density of 2.0×10^6 cells/ml and HEK293S GnTI$^-$ cells transfected at density of 20×10^6 cells/ml with transfection complex formed *a priori* (gray) or *in situ* (magenta) was monitored 3 dpt; error bars – standard deviations (one experiment performed in triplicate). (For interpretation of the references to color in this figure legend, the reader is referred to the web version of this article.)

viable cells (Fig. 2B). While the yield of model secreted protein was still quite lower when compared to our routine protocol with HEK293T cells (such trend is not unusual for HEK293S GnTI$^-$ cell line and was observed in previous studies [13]), it was still substantially increased when compared to the original low density transfection protocol (Fig. 2A). Furthermore, we compared both the *a priori* and *in situ* approach for formation of DNA:PEI transfection complexes in small scale (Fig. 2) and found the effect of both these approaches comparable with the *a priori* approach giving slightly better results. This is in very good agreement with previously reported higher yields with *a priori* complex formation [15,25].

High-density transfection of HEK293S GnTI$^-$ cells has comparable yield for a priori and in situ DNA:PEI complex formation

To confirm our results on non-model secreted protein we have used our optimized high-density transfection protocol for production of mutant LLT1(H176C) ectodomain in HEK293S GnTI$^-$ cells at 400 ml scale. We have further investigated the effect of *a priori* and *in situ* approach for transfection complexes formation at this scale as well as the effect of Freestyle F17 as the medium for incubation of cells at high density during the transfection. Unlike to the transfection at low cell density (data not shown) we were able to recover substantial amount of recombinant protein using the high-density transfection, routinely yielding approx. 3 mg per liter of HEK293S GnTI$^-$ production culture. And in agreement with the previous data we recovered higher yields with the *a priori* transfection complexes approach (Fig. 3A). However, we found that the high-density transfection in Freestyle F17 media with *a priori* complex formation is performing quite worse than in the EX-CELL293 – about 2-fold decrease in yield was observed (Fig. 3A). Based on these results we can recommend transfecting the suspension adapted HEK293S GnTI$^-$ cells in EX-CELL293 using the *a priori* approach, although we recognize that the *in situ* approach would be more suitable at even larger production scale, e.g. in bioreactor where it would allow for sequential addition of DNA and lPEI solutions through sterile filter equipped inlet ports (DNA:lPEI polyplexes cannot be sterile filtered).

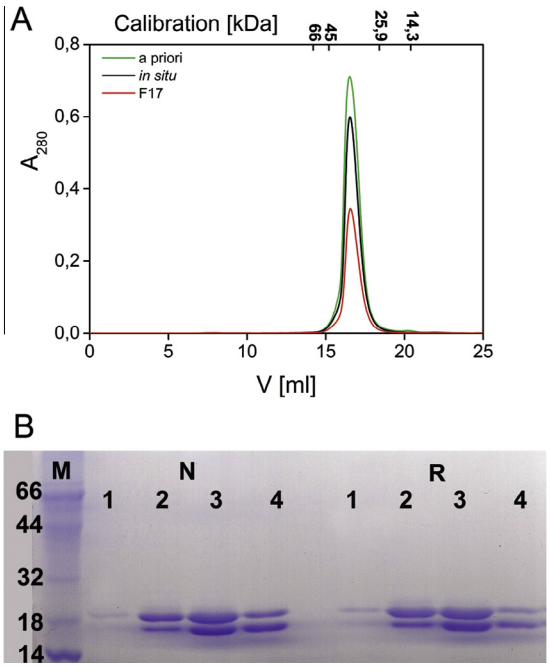

Fig. 3. EX-CELL293 medium is suitable for high-density transfection of HEK293S GnTI$^-$ cell line. (A) Size exclusion chromatography profiles of LLT1(H176C) protein purified from cell culture supernatants of HEK293S GnTI$^-$ cells transfected at 20×10^6 cells/ml in Freestyle F17 medium (red) or in EX-CELL293 medium with *a priori* (green) or *in situ* (black) transfection complexes formation; position of elution peaks of protein molecular weight standards is shown on the top axis. (B) Representative SDS–PAGE analysis of elution peak fractions from size exclusion chromatography analyzed under non-reducing (N) and reducing (R) conditions; M – molecular weight standards in kDa. (For interpretation of the references to color in this figure legend, the reader is referred to the web version of this article.)

LLT1 forms non-covalent dimer in solution independently of its N-glycans

While on SDS–PAGE, under both reducing and non-reducing conditions, the soluble LLT1(H176C) mutant migrates as two distinct monomeric glycoforms (Fig. 3B), SEC on Superdex 200 10/300 GL column used as final purification step suggested that LLT1(H176C) soluble ectodomain elutes as a non-covalent dimer (Fig. 3A). This finding was further corroborated using sedimentation equilibrium analysis in analytical ultracentrifuge (Fig. 4A). Fitting the data with the single ideal species model yielded a weight average molecular weight of 35,500 ± 500 Da which is in good agreement with a theoretical 36,191 Da weight of LLT1(H176C) dimer (including $GlcNAc_2Man_5$ oligosaccharides at both N-glycosylation sites), especially given the partial occupancy of the N-glycosylation sites. This observation is in contrast to previously published data for *E. coli* expressed and refolded LLT1(H176C) ectodomain obtained via SEC suggesting monomeric soluble protein [11].

We were therefore interested whether the presence of glycosylation might be the reason for dimer association. Towards this end we performed deglycosylation of various forms of LLT1 soluble ectodomain with endoglycosidase F1 [26]. As could be seen from SDS–PAGE analysis performed under non-reducing conditions, wild-type LLT1 ectodomain (fraction taken from the peak at 16 ml position on SEC run shown in Fig. 1B) forms besides monomer also a disulfidic dimer of approx. 40 kDa (Fig. 4C, lane WT), most probably an artifact caused by mixed disulfide pairing due to the presence of odd cysteine residue. For LLT1(H176C) mutant only monomer is observed, with N-glycans heterogeneity dramatically reduced when expressed in HEK293S GnTI$^-$ cells, allowing also for complete protein deglycosylation (Fig. 4C, lanes GnTI$^-$ and GnTI^-_D, respectively). However, sedimentation equilibrium analysis of deglycosylated protein (Fig. 4B) yielded weight average molecular weight of 32,400 ± 500 Da, again pointing for non-covalent dimer (theor. 32,135 Da for deglycosylated protein dimer). It should be noted that molecular weights derived from sedimentation equilibrium analysis are far more precise than that from SEC since it is direct thermodynamical method not dependent on calibration or interaction with column matrice. Also, the closest homologs of LLT1 from *clec2* gene family, i.e. CD69 and KACL, were found to form non-covalent dimers in solution and dimerization of KACL is presumed to increase affinity towards its monomeric ligand [27,28]. Furthermore, the prepared soluble LLT1(H176C) mutant with homogeneous $GlcNAc_2Man_5$ N-glycans (although still being inhomogeneous with respect to incomplete N-glycosylation site occupancy) was readily crystallized using the vapor diffusion method in sitting drop, forming hexagonal 3D rods (Fig. 4D) up to 150 μm in size. These primary crystals already provided protein diffraction up to resolution of 3.2 Å and were later optimized leading to solution of LLT1 crystal structure [29].

Conclusions

To conclude, we have optimized high-density transfection protocol for suspension adapted HEK293S GnTI$^-$ cell line and used it

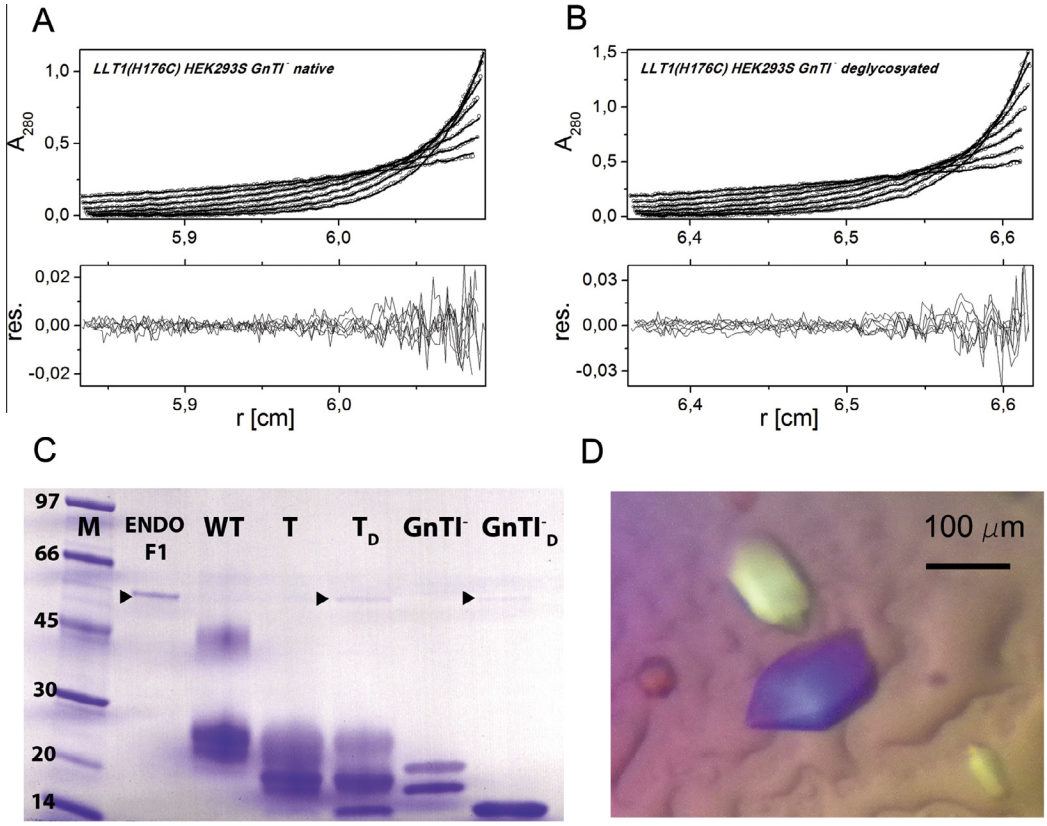

Fig. 4. LLT1(H176C) protein forms non-covalent dimer in solution, is easily deglycosylated and crystallizes. (A) and (B) Sedimentation equilibrium analysis in analytical ultracentrifuge has shown that both native and deglycosylated LLT1(H176C) produced in HEK293S GnTI⁻ cells behaves as non-covalent homodimer in solution; upper panels – absorbance data with fitted curves (single non-interacting discrete species model), lower panels – residual plot showing the goodness of fit. (C) SDS–PAGE analysis of LLT1(H176C) deglycosylation under non-reducing conditions; M – molecular weight standards in kDa, ENDO F1 – endoglycosidase F1 used for deglycosylation (arrow), WT – wild-type LLT1 produced in HEK293T cells, T and T_D – native and deglycosylated LLT1(H176C) produced in HEK293T cells, GnTI⁻ and $GnTI^-_D$ – native and deglycosylated LLT1(H176C) produced in HEK293S GnTI⁻ cells. (D) Crystals of native LLT1(H176C) protein produced in HEK293S GnTI⁻ cell line.

for production of LLT1(H176C) mutant ectodomain that forms stable, deglycosylatable and crystallizable non-covalent homodimer in solution which formation is not dependent upon presence of N-glycans. To our knowledge, this is the first attempt at structural characterization of human LLT1 immunoreceptor. The strategy of construct design described herein for LLT1 – i.e. the restoration of disulfidic bond pairing pattern – might be considered also for other C-type lectin-like receptors of NK cells, either for protein production aimed at structural characterization or for production of stable soluble receptor domains that could be utilized in clinical therapy. Apart from LLT1, the high-density transfection protocol described here was within our laboratory successfully used for production of different soluble receptor domains as well as other recombinant proteins and is generally applicable for protein production within HEK293S GnTI⁻ cell line, especially for protein crystallography.

Acknowledgments

We thank Dr. Yves Durocher for the pTT28, pTTo3c_SSH and pTTo_GFPq plasmids and Dr. Radu A. Aricescu for HEK293T cell line. This work was supported by Charles University in Prague (GAUK 403211/2010, UNCE 204025/2012, SVV 260079/2014), High Education Development Fund (FRVS 669/2013), Institutional Research Concept of the Institute of Microbiology (RVO61388971) and grants from Ministry of Education, Youth and Sports of the Czech Republic and European Regional Development Funds (CZ.1.07/2.3.00/30.0003 and CZ.1.05/1.1.00/02.0109). Access to instrumental and other facilities was supported by EU (Operational Program Prague – Competitiveness project CZ.2.16/3.1.00/24023). The research leading to these results has received funding from the European Community's Seventh Framework Programme (FP7/2007-2013) under BioStruct-X (grant agreement N°283570) and from Instruct, part of the European Strategy Forum on Research Infrastructures (ESFRI) supported by national member subscriptions.

Appendix A. Supplementary data

Supplementary data associated with this article can be found, in the online version, at http://dx.doi.org/10.1016/j.pep.2015.01.006.

References

[1] E. Vivier, E. Tomasello, M. Baratin, T. Walzer, S. Ugolini, Functions of natural killer cells, Nat. Immunol. 9 (2008) 503–510.
[2] T.I. Arnon, G. Markel, A. Bar-Ilan, J. Hanna, E. Fima, F. Benchetrit, R. Galili, A. Cerwenka, D. Benharroch, N. Sion-Vardy, A. Porgador, O. Mandelboim, Harnessing soluble NK cell killer receptors for the generation of novel cancer immune therapy, PLoS One 3 (2008) e2150.
[3] C. Kellner, T. Maurer, D. Hallack, R. Repp, J.G. van de Winkel, P.W. Parren, T. Valerius, A. Humpe, M. Gramatzki, M. Peipp, Mimicking an induced self phenotype by coating lymphomas with the NKp30 ligand B7–H6 promotes NK cell cytotoxicity, J. Immunol. 189 (2012) 5037–5046.
[4] C. Germain, F. Bihl, S. Zahn, G. Poupon, M.J. Dumaurier, H.H. Rampanarivo, S.B. Padkjaer, P. Spee, V.M. Braud, Characterization of alternatively spliced transcript variants of CLEC2D gene, J. Biol. Chem. 285 (2010) 36207–36215.

[5] C. Germain, A. Meier, T. Jensen, P. Knapnougel, G. Poupon, A. Lazzari, A. Neisig, K. Hakansson, T. Dong, N. Wagtmann, E.D. Galsgaard, P. Spee, V.M. Braud, Induction of lectin-like transcript 1 (LLT1) protein cell surface expression by pathogens and interferon-gamma contributes to modulate immune responses, J. Biol. Chem. 286 (2011) 37964–37975.
[6] H. Aldemir, V. Prod'homme, M.J. Dumaurier, C. Retiere, G. Poupon, J. Cazareth, F. Bihl, V.M. Braud, Cutting edge: lectin-like transcript 1 is a ligand for the CD161 receptor, J. Immunol. 175 (2005) 7791–7795.
[7] D.B. Rosen, J. Bettadapura, M. Alsharifi, P.A. Mathew, H.S. Warren, L.L. Lanier, Cutting edge: lectin-like transcript-1 is a ligand for the inhibitory human NKR-P1A receptor, J. Immunol. 175 (2005) 7796–7799.
[8] P. Roth, M. Mittelbronn, W. Wick, R. Meyermann, M. Tatagiba, M. Weller, Malignant glioma cells counteract antitumor immune responses through expression of lectin-like transcript-1, Cancer Res. 67 (2007) 3540–3544.
[9] S. Satkunanathan, N. Kumar, M. Bajorek, M.A. Purbhoo, F.J. Culley, Respiratory syncytial virus infection, TLR3 ligands, and proinflammatory cytokines induce CD161 ligand LLT1 expression on the respiratory epithelium, J. Virol. 88 (2014) 2366–2373.
[10] A.N. Zelensky, J.E. Gready, The C-type lectin-like domain superfamily, FEBS J. 272 (2005) 6179–6217.
[11] J. Kamishikiryo, H. Fukuhara, Y. Okabe, K. Kuroki, K. Maenaka, Molecular basis for LLT1 protein recognition by human CD161 protein (NKRP1A/KLRB1), J. Biol. Chem. 286 (2011) 23823–23830.
[12] P.J. Reeves, N. Callewaert, R. Contreras, H.G. Khorana, Structure and function in rhodopsin: high-level expression of rhodopsin with restricted and homogeneous N-glycosylation by a tetracycline-inducible N-acetylglucosaminyltransferase I-negative HEK293S stable mammalian cell line, Proc. Natl. Acad. Sci. U.S.A. 99 (2002) 13419–13424.
[13] Y. Zhao, B. Bishop, J.E. Clay, W. Lu, M. Jones, S. Daenke, C. Siebold, D.I. Stuart, E.Y. Jones, A.R. Aricescu, Automation of large scale transient protein expression in mammalian cells, J. Struct. Biol. 175 (2011) 209–215.
[14] A.R. Aricescu, W. Lu, E.Y. Jones, A time- and cost-efficient system for high-level protein production in mammalian cells, Acta Crystallogr. D Biol. Crystallogr. 62 (2006) 1243–1250.
[15] G. Backliwal, M. Hildinger, V. Hasija, F.M. Wurm, High-density transfection with HEK-293 cells allows doubling of transient titers and removes need for a priori DNA complex formation with PEI, Biotechnol. Bioeng. 99 (2008) 721–727.
[16] D.L. Hacker, D. Kiseljak, Y. Rajendra, S. Thurnheer, L. Baldi, F.M. Wurm, Polyethyleneimine-based transient gene expression processes for suspension-adapted HEK-293E and CHO-DG44 cells, Protein Expr. Purif. 92 (2013) 67–76.
[17] C. Raymond, R. Tom, S. Perret, P. Moussouami, D. L'Abbe, G. St-Laurent, Y. Durocher, A simplified polyethylenimine-mediated transfection process for large-scale and high-throughput applications, Methods 55 (2011) 44–51.
[18] Y. Durocher, S. Perret, A. Kamen, High-level and high-throughput recombinant protein production by transient transfection of suspension-growing human 293-EBNA1 cells, Nucleic Acids Res. 30 (2002) E9.
[19] R. Higuchi, B. Krummel, R.K. Saiki, A general method of in vitro preparation and specific mutagenesis of DNA fragments: study of protein and DNA interactions, Nucleic Acids Res. 16 (1988) 7351–7367.
[20] S.N. Ho, H.D. Hunt, R.M. Horton, J.K. Pullen, L.R. Pease, Site-directed mutagenesis by overlap extension using the polymerase chain reaction, Gene 77 (1989) 51–59.
[21] P.L. Pham, S. Perret, B. Cass, E. Carpentier, G. St-Laurent, L. Bisson, A. Kamen, Y. Durocher, Transient gene expression in HEK293 cells: peptone addition posttransfection improves recombinant protein synthesis, Biotechnol. Bioeng. 90 (2005) 332–344.
[22] P. Schuck, On the analysis of protein self-association by sedimentation velocity analytical ultracentrifugation, Anal. Biochem. 320 (2003) 104–124.
[23] P. Pompach, P. Man, D. Kavan, K. Hofbauerova, V. Kumar, K. Bezouska, V. Havlicek, P. Novak, Modified electrophoretic and digestion conditions allow a simplified mass spectrometric evaluation of disulfide bonds, J. Mass Spectrometry 44 (2009) 1571–1578.
[24] M.M. Young, N. Tang, J.C. Hempel, C.M. Oshiro, E.W. Taylor, I.D. Kuntz, B.W. Gibson, G. Dollinger, High throughput protein fold identification by using experimental constraints derived from intramolecular cross-links and mass spectrometry, Proc. Natl. Acad. Sci. U.S.A. 97 (2000) 5802–5806.
[25] E.J. Schlaeger, K. Christensen, Transient gene expression in mammalian cells grown in serum-free suspension culture, Cytotechnology 30 (1999) 71–83.
[26] F. Grueninger-Leitch, A. D'Arcy, B. D'Arcy, C. Chene, Deglycosylation of proteins for crystallization using recombinant fusion protein glycosidases, Protein Sci. 5 (1996) 2617–2622.
[27] O. Vanek, M. Nalezkova, D. Kavan, I. Borovickova, P. Pompach, P. Novak, V. Kumar, L. Vannucci, J. Hudecek, K. Hofbauerova, V. Kopecky Jr., J. Brynda, P. Kolenko, J. Dohnalek, P. Kaderavek, J. Chmelik, L. Gorcik, L. Zidek, V. Sklenar, K. Bezouska, Soluble recombinant CD69 receptors optimized to have an exceptional physical and chemical stability display prolonged circulation and remain intact in the blood of mice, FEBS J. 275 (2008) 5589–5606.
[28] Y. Li, Q. Wang, S. Chen, P.H. Brown, R.A. Mariuzza, Structure of NKp65 bound to its keratinocyte ligand reveals basis for genetically linked recognition in natural killer gene complex, Proc. Natl. Acad. Sci. U.S.A. 110 (2013) 11505–11510.
[29] T. Skalova, J. Blaha, K. Harlos, J. Duskova, T. Koval, J. Stransky, J. Hasek, O. Vanek, J. Dohnalek, Four crystal structures of human LLT1, a ligand for human NKR-P1, in varied glycosylation and oligomerization state, *Acta Crystallogr. D Biol. Crystallogr.* (in press).